International Scientific Colloquium
Modelling for Material Processing
Riga, September 16-17, 2010

Modelling of Cavitation and Bubble Growth During Ultrasonic Cleaning Process

T. Sile, J. Virbulis, A. Timuhins, J. Sennikovs, U. Bethers

Abstract

The model explaining bubble growth during pulsed ultrasound processing is presented. The rectified diffusion, bubble dissolution, buoyancy rising and bubble coalescence due to the secondary Bjerknes force are considered. The model is calibrated using experimental data and parameter studies are carried out.

Introduction

Ultrasound is used for the cleaning of silicon wafers from nanosize particles. Although the cleaning process and many phenomena occurring in cleaning baths have been experimentally established, the precise mechanism of particle removal is unclear. Recent experimental results suggest that cavitation bubbles have a significant role in this process [1]. The process of particle removal is linked with bubble oscillations in acoustic field, which depend heavily on the equilibrium bubble radius [2, p.310]. Therefore, to improve the cleaning process, it is necessary to determine the equilibrium bubble size distribution in the cleaning liquid.

High intensity ultrasound creates cavitation bubbles that collapse violently. The bubbles contain mainly air and a relatively small amount of water vapour. The oscillating bubbles absorb and scatter ultrasound energy. The dynamics of bubble oscillations can be described by the Keller-Miksis model and depends on such parameters as the equilibrium bubble radius, the frequency and the intensity of the acoustic field, etc. [3].

The initial concentration distribution of gas bubbles in water is reported by many authors, e.g. [4, 5], and it is similar for water under different conditions. Typically, the number of bubbles is inversely proportional to the third power of the bubble radius. It is not clearly known why the small gas bubbles can exist in the water for a long time, because they should disappear due to surface tension, however, different hypothesis to explain this have been proposed [5, 6, 7, 8].

The equilibrium bubble radius which is unequivocally linked with the amount of gas in the bubble can change over time. One of the causes is rectified diffusion – the exchange of gas between bubble and surrounding liquid caused by changes in gas pressure when the bubble oscillates. Bubbles can coalesce due to attractive Bjerknes forces and consequently create larger bubbles. The process of rectified diffusion has been extensively studied; however a quantitative description of bubble coalescence and bubble generation on the surfaces of the vessel has yet to be proposed.

Therefore the bubble radius distribution after the treatment of water with ultrasound is unclear and experimental results contradict each other [9, 10].

Clear experimental data is needed for the model development. We consider the experiments of Iida et al. [11, 12]. The authors measured the bubble distribution using Fraunhofer laser diffraction and pulsed ultrasound with frequency 443 kHz (transducer

switched on for 10000 acoustic cycles and off for 20000 cycles in each pulse). A basic model was used to explain these experiments [12] – the model included bubble generation, dissolution and coalescence; however it could not replicate all features of the experimental data: bubble growth does not stop after 15 pulses as can be seen in the experiments [11] and the peak of bubble size distributions is wider in experiments.

We propose a model based on expressions for the secondary Bjerknes force, calibrate this model against the Iida experiments and investigate the growth and shrinkage of the bubble population under different conditions.

1. Model

The range of bubble radius from 10^{-7} to 10^{-4} m was divided into 200 logarithmically distributed bins for the calculations.

The dynamics of a single bubble are described by the Keller-Miksis (KM) equation [3]:

$$\left(1-\frac{\dot{R}}{c}\right)R\ddot{R}+\frac{3}{2}\dot{R}^2\left(1-\frac{\dot{R}}{3c}\right)=\left(1+\frac{\dot{R}}{c}\right)\frac{p_l}{\rho}+\frac{R}{\rho c}\frac{dp_l}{dt},$$

$$p_l=\left(p_0+\frac{2\sigma}{R_0}\right)\left(\frac{R_0}{R}\right)^{3\kappa}-p_0-\frac{2\sigma}{R}-\frac{4\mu}{R}\dot{R}-p_a(t)\,,$$

where R – bubble radius, c – speed of sound, overdots denote the time derivative, ρ – liquid density, σ – surface tension, R_0 – equilibrium bubble radius, κ – polytropic constant, p_0 – ambient pressure, μ – viscosity, p_a – acoustic pressure, t – time.

Typically bubble oscillations are the most prominent if equilibrium radius of the bubble is in the vicinity of resonant radius determined by the frequency of the acoustic field *f* (Minnaert's formula) [2, p. 139]:

$$fR_r=3\left[\frac{m}{s}\right].$$

If no acoustic pressure is applied, bubbles gradually lose gas because the pressure inside the bubble is higher than outside the bubble. Bubble dissolution is described by the following equation [2, pp.383]:

$$\dot{R_0}=\frac{C_0D}{\rho_{gas}}\left(\frac{C_\infty}{C_0}-1-\frac{2\sigma}{p_0R_0}\right)\left(\frac{1}{R_0}+\frac{1}{\sqrt{\pi Dt}}\right),$$

where – C_0 – gas saturation concentration, D – gas diffusion coefficient, C_∞- gas concentration in the liquid far from the bubble.

Rectified diffusion is described by the following equation [2, pp. 397]:

$$\dot{R_0}=\frac{DR_gTC_0}{p_0R_0\left(1+\frac{4\sigma}{3p_0R_0}\right)}\left(\left\langle\frac{R}{R_0}\right\rangle+R_0\sqrt{\frac{\left\langle\frac{R^4}{R_0^4}\right\rangle}{\pi Dt}}\right)\left(\frac{C_\infty}{C_0}-\frac{\left\langle\frac{R^4}{R_0^4}\cdot\frac{p_g}{p_0}\right\rangle}{\left\langle\frac{R^4}{R_0^4}\right\rangle}\right),$$

where R_g – universal gas constant, T – absolute temperature, $<\cdot>$ denotes time average, p_g – gas pressure inside the bubble.

The time averaged coefficients are calculated numerically by solving the KM equation for each bubble radius and averaging over 100 periods after 900 periods of transition time.

The number of bubbles moved to another bin is determined as follows: first, the change in bubble radius for a bubble with a radius corresponding to the middle of the bin is calculated, and then the percentage of bubbles moved away from the bin is calculated dividing the change in the radius with the difference between the endpoints of the bin.

The attraction between two bubbles (with indices *1* and *2*) is described using the secondary Bjerknes force $FB2_{12}$ [13]:

$$FB2_{12} = \frac{\rho \cdot R_1 \left(2\dot{R_1}^2 + R_1\ddot{R}_1\right)}{d_{12}^2} \cdot \frac{4}{3}\pi R_2^3,$$

where d – distance between bubbles.

We assume that only bubbles with the same radius are attracted and the bubble motion is described by the following equation for the bubble position x:

$$\frac{1}{2}\rho \cdot V_0 \cdot \ddot{x}(t) = -\frac{\rho \cdot R\left(2\dot{R}^2 + R\ddot{R}\right)}{\left(2x(t)\right)^2} \cdot \frac{4}{3}\pi R^3,$$

where V_0 – equilibrium bubble volume. The numerically calculated values of secondary Bjerknes force using parameters from Iida's experiments and different values of acoustic pressure amplitude are shown in Fig. 1. Results show that the secondary Bjerknes force depends significantly on bubble radius reaching maximum near the resonance and decreasing for bubbles larger and smaller than the resonant bubble radius.

By integrating this equation we obtain the coalescence time for two bubbles at a distance of $2x_0$

$$t(x \to 0) = \frac{\pi}{\sqrt{2}}\frac{\sqrt{x_0}x_0}{\sqrt{k}},$$

where

$$k = \frac{8\pi R^4\left(2\dot{R}^2 + R\ddot{R}\right)}{3V_0}.$$

Assuming a uniform bubble distribution, typical half distance between two bubbles can be approximated as:

$$x_0 = \frac{1}{2} \cdot C_b^{-\frac{1}{3}},$$

where C_b – bubble concentration.

The probability of two bubbles coalescing in a given amount of time is inversely proportional to the time needed for coalescence. However, bubble dynamics is complicated and an attractive force between bubbles does not always result in coalescence [14], therefore we introduce a constant calibration coefficient h (see below).

The acoustic energy is dissipated on the bubbles therefore at larger bubble concentration the acoustic energy in the same spatial position is smaller and bubble growth rate is reduced. Absorption is described after Krasilnikov [15]. Depending on the bubble concentration, the absorption, acoustic pressure and the secondary Bjerknes force are recalculated at each time step. The measurement point in Iida's experiments is located 7.5 cm from the transducer and we assume a uniform bubble distribution in the entire volume and an exponential decay of acoustic energy from the transducer to the measurement point.

In Iida's model the number of coalescing bubbles C_c in the i-th bin is calculated as

$$C_c^i = P_c \cdot C_b^i,$$

where coalescence probability is

$$P_c = h \cdot \frac{C_b^i}{\sum_i C_b^i}.$$

Combining all these effects we propose to change the coalescence probability in the following way

$$P_c = h \cdot \sqrt{C_b^i}\sqrt{k_a},$$

and h – calibration parameter, k_a – the secondary Bjerknes force parameter k modified to account for absorption.

For bubble generation we use Iida's approach – a constant bubble volume is generated for each bubble bin smaller than the resonant radius at each time step.

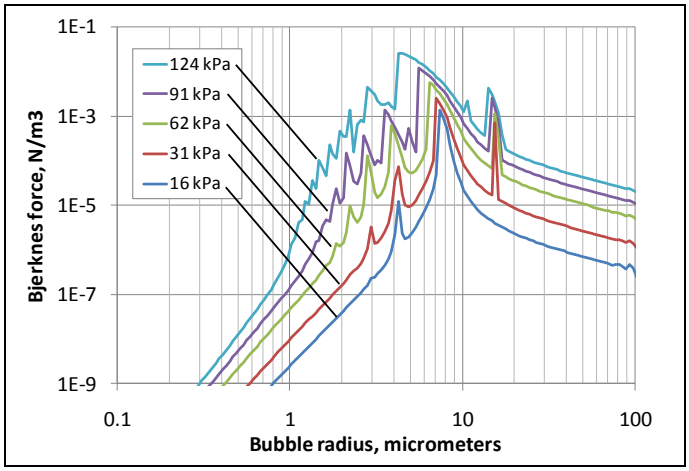

Fig. 1. Numerically calculated Bjerknes force for different values of acoustic pressure amplitude

Large bubbles rise to the water surface due to buoyancy and leave the system. We consider this degasification effect introducing a negative source term in each bubble bin

$$R^i = -C_b^i \cdot 2v_S\,/H,$$

where v_S is Stokes velocity and H is the height of water tank.

For clarity, calculations using this model are denoted "SRBC" (Square Root of the Bjerknes force and Concentration).

2. Results

The main parameters used in simulation are as follows: frequency - 443 kHz, acoustic pressure - 124 kPa, gas saturation - 90%. The model calibration is performed by changing the coalescence coefficient h to minimize the sum of the quadratic differences between experimental and modelled average bubble radius during pulses 2, 5, 8, 11 and 14. The optimal value of the coalescence coefficient h is $4 \cdot 10^{-5}$, i.e. as expected smaller than 1. The experimental and modelled bubble volume probabilities during pulses 2, 5 and 8 are shown in Fig. 2. The average bubble radius (radius, at which 50% of total bubbles volume is concentrated in smaller bubbles) as a function of pulse number for experimental data, Iida's model and SRBC model is shown in Fig. 3. The SRBC model describes the experimental behaviour better than the Iida's model; however, the saturation is not reached after 15 pulses.

The experiment with different ON/OFF time ratios of ultrasonic energy [11] is used for verification of SRBC model. The average bubble radius after 15 ON/OFF pulses from

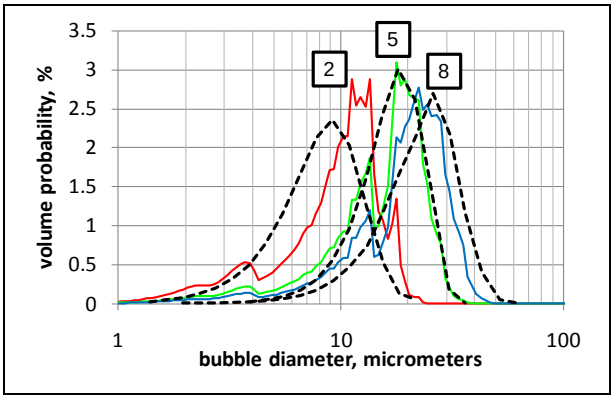

Fig. 2. Experimental (dotted) and modelled bubble volume probabilities during pulses 2, 5 and 8

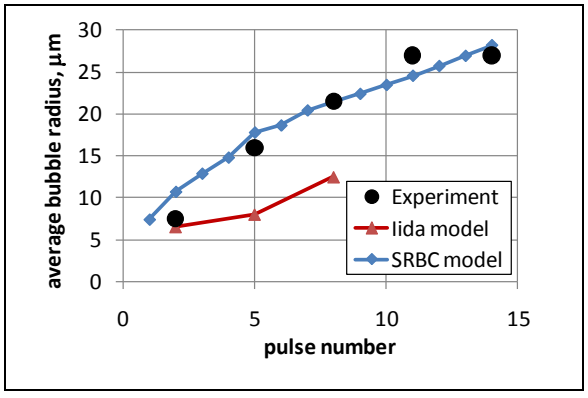

Fig. 3. Average bubble radius as a function of pulse number for experimental data, Iida model and SRBC model

SRBC model and Iida's model, as well as

experimental equilibrium average bubble size [11] are plotted in Fig. 4. Also for this experiment the agreement with SRCB model is better than with Iida's model.

The effect of bubble rising due to buoyancy is shown in Fig. 5. The curve corresponding to simulations without bubble rise is denoted with "0", with rise - "1". The results with rising show saturation of average bubble radius after 100 pulses. To account for additional causes responsible for bubble escape from the system (radiation force, acoustic streaming etc.) we calculate another two cases, increasing the bubble rising term by a factor of 10 and 20. The latter case fits the experimental data well and therefore the escape of bubbles from the system can be a possible explanation for saturation.

In typical cleaning process the sonification is continuous or has a pulse length of a few seconds. Therefore we simulated a system that undergoes 10 s of sonification (ON) followed by 20 s without sonification (OFF). The average bubble radius and the total volume of bubbles for two cases with different gas saturation levels - C_∞/C_0 =0.9 and 0.1 are shown in Fig. 6. For parameters used the steady state bubble distribution arises after 5 s. When the acoustic field is turned off, the total bubble volume and average radius decreases approx. by a factor of two during the next 2 s. Fig. 7 shows the volume distribution at 1 s, 2 s and 10 s after turning the acoustic field ON, as well as at 1 s and 10 s after switching the acoustic field OFF. The distribution has two maxima – under (~0.5 μm) and over (~100 μm) resonance radius (~7 μm). The maximum corresponding to smaller bubbles disappears after 0.1 s. The graph shows that the gas content has a minor influence during ON time, because coalescence dominates

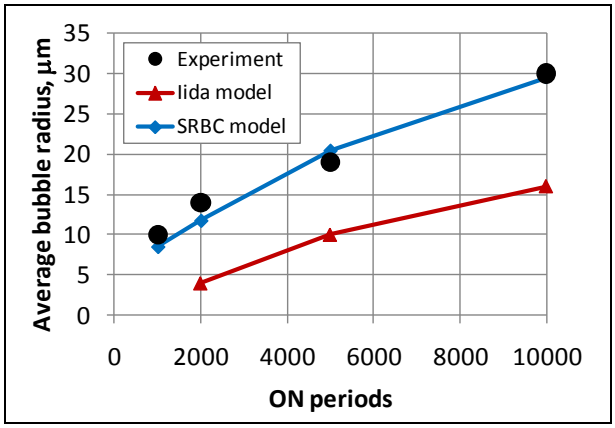

Fig. 4. Experimental data (dots), Iida model (triangles) and SRBC model after 15 pulses for different number of ON periods in pulse

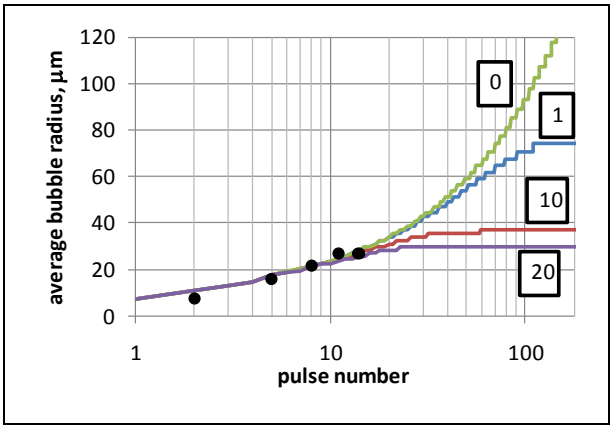

Fig. 5. The effect of bubble rising: numbers denote the multiplier at rising term; dots – experimental data

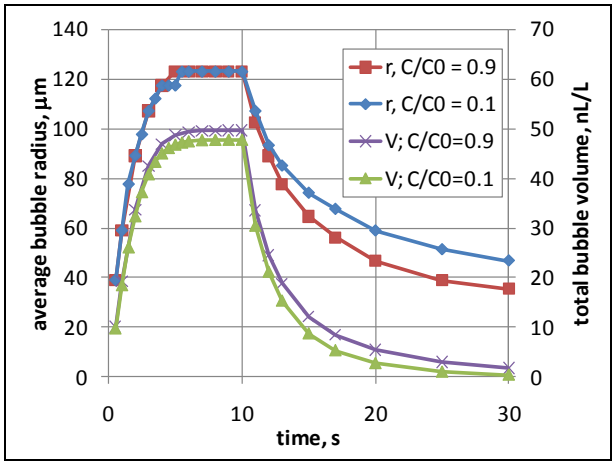

Fig. 6. Average bubble radius r and total volume *V* for process 10 s on - 20 s off. Dissolved gas concentration C_∞/C_0 = 0.1 and 0.9

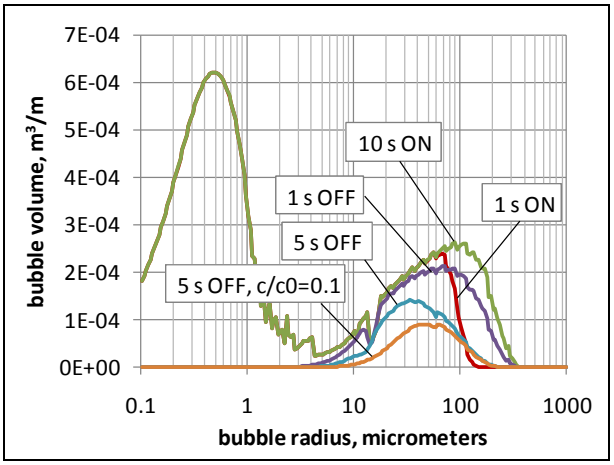

Fig. 7. Bubble volume distribution at 5 time moments for process 10 s on – 20 s off

over the rectified diffusion. During the OFF time the main reason for the decrease of average radius and total volume of bubbles is the rising of bubbles due to buoyancy. The dissolution of bubbles has also considerable effect, especially for smaller bubbles and degassed water.

Conclusions

We have improved the bubble growth model proposed by Iida describing bubble coalescence using the secondary Bjerknes force that depend on bubble radius and are numerically calculated using the Keller-Miksis bubble dynamics equations. The buoyant rising of bubbles is added to the SRBC model. The SRBC model shows a better agreement with the experimental data. The results show the coalescence to be the main cause of bubble growth which is consistent with results obtained by Iida and the dissolution and the buoyant rising to be the main factors of bubble reduction.

Acknowledgement

The research was carried out with the financial support from ESF project at Latvia University with contract No.: 2009/0223/1DP/1.1.1.2.0/09/APIA/VIAA/008.

References

[1] Kim, W., Kim, T.-H., Choi, J., Kim, H.-Y.: *Mechanism of particle removal by megasonic waves.,* Appl. Phys. Lett., 2009, Vol. 94, pp. 081908.
[2] Leighton T.G.: *The Acoustic Bubble.* Academic Press, 1997, 613 pp.
[3] Parlitz, U., Mettin, R., Luther, S., Akhatov, I., Voss, M., Lauterborn, W.: *Spatio-temporal dynamics of acoustic cavitation bubble clouds.* Phil. Trans. R. Soc. Lond. A., Vol. 357, 1999, pp. 313-334.
[4] Liu, Z., Sato, K., Brennen, C.E.: *Cavitation nuclei population dynamics in a water tunel.* ASME Cavitation and Multiphase Flow Forum, 1993. Fluids Engineering Division, FED-153
[5] Brennen, C.E.: *Cavitation and Bubble Dynamics.* Oxford University Press, New York, 1995.
[6] Margulis, M.A.: *Sonochemistry and cavitation.* Gordon and Breach Publishers, 1995.
[7] Potter, J. R.: *A possible mechanism for acoustic triggering of decompression sickness symptoms in deep-diving marine mammals.* Proc. of the 2004 Int. Symposium on Underwater Technology, 2004
[8] Mørch, K. A.: *Reflections on cavitation nuclei in water.* Phys. Fluids, Vol. 19, 2007, pp. 072104.
[9] Ashokkumar, M., Lee, J., Kentish, S.: *Bubbles in an acoustic field: An overview,* Ultrasonics Sonochemistry, Vol. 14, 2007, pp. 470-475.
[10] Choa, S.-H., Kimb, J.-Y., Chuna, J.-H., Kim, J.-D.: *Ultrasonic formation of nanobubbles and their zeta-potentials in aqueous electrolyte and surfactant solutions.* Colloids and Surfaces A: Physicochemical and Engineering Aspects, Vol. 269, 2005, pp. 28-34
[11] Iida, Y., Ashokkumar, M., Tuziuti, T., Kozuka, T., Yasui, K., Towata, A., Lee, J.: *Bubble population phenomena in sonochemical reactor: I Estimation of bubble size distribution and its number density with pulsed sonication – Laser diffraction method.* Ultrasonics Sonochemistry, Vol. 17, 2010, pp. 473–479.
[12] Iida, Y., Ashokkumar, M., Tuziuti, T., Kozuka, T., Yasui, K., Towata, A., Lee, J.: *Bubble population phenomena in sonochemical reactor: II. Estimation of bubble size distribution and its number density by simple coalescence model calculation.* Ultrasonics Sonochemistry, Vol. 17, 2010, pp. 480–486.
[13] Mettin, R., Akhatov, I., Parlitz, U., Ohl, C.D., Lauterborn, W.: *Bjerknes forces between small cavitation bubbles in a strong acoustic field.* Physical Review E, Vol.56, 1997, No.3, pp. 2924-2931.
[14] Doinikov A.A.: *Translational motion of two interacting bubbles in a strong acoustic field,* Physical Review E, Vol.64, 2001, pp. 026301.
[15] Krasilnikov, V.A., Krylov, V.V.: *Vvedenie v fizicheskuyu akustiku (Introduction to Physical Acoustics),* Nauka, Moscow, 1984 (in Russian).

Authors

Sile, Tija
Dr.-Phys. Virbulis, Janis
Timuhins, Andrejs
Sennikovs, Juris
Dr.-Phys. Bethers, Uldis

Faculty of Physics and Mathematics
University of Latvia
Zellu str. 8
LV-1002 Riga, Latvia
E-mail: janis@modlab.lv